Dominant mechanisms for the delivery of fine sediment and phosphorus to fluvial networks draining grassland dominated headwater catchments

M.T. Perks[a*], G.J. Owen[b], C.McW.H. Benskin[c], J. Jonczyk[b], C. Deasy[c,d,e], S. Burke[f], S.M. Reaney[d], P.M. Haygarth[c]

[a] School of Geography Politics and Sociology, Newcastle University, Newcastle upon Tyne NE1 7RU, United Kingdom

[b] School of Civil Engineering and Geosciences, Newcastle University, Newcastle upon Tyne NE1 7RU, United Kingdom

[c] Lancaster Environment Centre, Lancaster University, Lancaster LA1 4YQ, United Kingdom

[d] Department of Geography, Durham University, Durham DH1 3LE, United Kingdom

[e] Northumbrian Water Ltd., Boldon House, Wheatlands Way, Pity Me, Durham DH1 5FA, United Kingdom

[f] British Geological Survey, Environmental Science Centre, Nicker Hill, Keyworth, Nottingham NG12 5GG, United Kingdom*   Corresponding author

HIGHLIGHTS

• We assess how sediment and phosphorus is transported in an agricultural catchment

• Multiple pathways are observed for particulate and soluble constituents

• Delivery is complicated by dominance & variability of erosive processes & pathways

• Large challenges faced in mitigating delivery of contaminants to headwater rivers

Key words:

Fluvial; suspended sediment; phosphorus; diffuse pollution; water quality; headwater; connectivity; grassland

Abstract

Recent advances in monitoring technology have enabled high frequency, in-situ measurements of total phosphorus and total reactive phosphorus to be undertaken with high precision, whilst turbidity can provide an excellent surrogate for suspended sediment. Despite these measurements being fundamental to understanding the mechanisms and flow paths that deliver these constituents to river networks, there is a paucity of such data for headwater agricultural catchments. The aim of this paper is to deduce the dominant mechanisms for the delivery of fine sediment and phosphorus to an upland river network in the UK through characterisation of the temporal variability of hydrological fluxes, and associated soluble and particulate concentrations for the period spanning March 2012 - February 2013. An assessment of the factors producing constituent hysteresis is undertaken following Factor Analysis (FA) on a suite of measured environmental variables representing the fluvial and wider catchment conditions prior to, and during catchment-wide hydrological events. Analysis indicates that suspended sediment is delivered to the fluvial system predominantly via rapidly responding pathways driven by event hydrology. However, evidence of complex, figure-of-eight hysteresis is observed following periods of hydrological quiescence, highlighting the importance of preparatory processes. Sediment delivery via a slow moving, probably sub-surface pathway does occur, albeit infrequently and during low magnitude events at the catchment outlet. Phosphorus is revealed to have a distinct hysteretic response to that of suspended sediment, with sub-surface pathways dominating. However, high magnitude events were observed to exhibit threshold-like behaviour, whereby activation and connection of usually disconnected depositional zones to the fluvial networks results in the movement of vast phosphorus fluxes. Multiple pathways are observed for particulate and soluble constituents, highlighting the challenges faced in mitigating the delivery of contaminant fluxes to headwater river systems.

1 Introduction

Understanding the hydrological and pollutant dynamics of headwater catchments, and the implicit connections between the land and the river is of great importance (Bishop et al., 2008). These rivers account for 60 to 80% of the entire river network (Benda et al., 2005), providing potable drinking water (Sturdee et al., 2007), buffering capacity for flood risk (Posthumus et al., 2008), dilution of nutrient rich waters downstream (Bowes et al., 2003) and ecological habitats fundamental to the health of the aquatic ecosystems (Meyer et al., 2007). Maintaining the quality of headwater resources is thus essential for the sustainability of the water environment (Soulsby et al., 2002). A significant risk to the systems' functional integrity is the presence of surface sediment sources that are enriched with phosphorus (P) following years of excessive fertiliser inputs (Heathwaite et al., 2006; Withers et al., 2001; Withers et al., 2007), which may be exacerbated by land-use conflicts (Pacheco et al., 2014; Valle Junior et al., 2014) and accelerating rates of terrestrial erosion (Mainstone et al., 2008; McHugh, 2007). The delivery of these materials to hydrological networks is augmented by the relatively low filter resistance and restricted potential for temporary storage in these small catchments. Resultantly, the catchment export of sediment and P may be closely related to the magnitude of erosion and land degradation (Kovacs et al., 2012), with adverse impacts on the aquatic habitats ensuing (Collins and Walling, 2004; Haygarth et al., 2005a; Haygarth et al., 2005b; Holden et al., 2007; Valle Junior et al., 2015).

To moderate the number of watercourses failing to produce ecologically sustainable habitats as a result of enhanced erosion and delivery of pollutants to sensitive headwater fluvial networks, identification of the fine sediment and nutrient sources, and the pathways of delivery is firstly required (Jarvie et al., 2008), with management efforts subsequently focussing on restoring natural attenuation within catchments and disconnecting the identified Critical Source Areas (CSAs), or hot-spots from the fluvial networks (Heathwaite et al., 2005; Kovacs et al., 2012; Newson, 2010; Pionke et al., 1996). Many well established factors act to define the CSAs of fine sediment and P, however, our understanding of how and when these areas are connected to the fluvial networks is limited by the heterogeneity of factors governing process rates (Dean et al., 2009). These factors include antecedent moisture conditions, runoff mechanisms, spatial variation of rainfall intensity, and land management operations. These process controls influence the mechanisms of mobilisation, pathways of transfer, and the complex biogeochemical processes occurring along the land-water continuum, yet, they are diffuse, difficult to quantify at the catchment-scale, and vary on an

event basis. Understanding of how pollutant transmission varies in response to temporal and spatial constraints may however provide key information about connectivity of pollutant sources, pathways of delivery and pollutant transfer in a catchment (Lexartza-Artza and Wainwright, 2009).

A large amount of research has been conducted to improve our understanding of the timing and mechanisms responsible for the transport of aquatic pollutants in surface and sub-surface runoff from agricultural land, with investigations into the fluvial export of suspended sediment from small agricultural catchments enabling exploration of the processes responsible for its delivery (e.g. Glendell and Brazier, 2014; Steegen et al., 2000; Thompson et al., 2013). Likewise, studies have sought to characterise the nature of P losses from headwater agricultural catchments (e.g. Haygarth et al., 2005b; Hodgkinson and Withers, 2007; Pionke et al., 1996; Soulsby et al., 2002; Stutter et al., 2008). However, there is currently a dearth of continuous, high-temporal resolution hydro-chemical and suspended sediment monitoring datasets available for rivers draining sensitive headwater catchments. Such high-frequency datasets of discharge, suspended sediment (SS), total phosphorous (TP) and total reactive phosphorus (TRP) enable characterisation of the complex non-linear responses of the monitored determinands at sub-hourly timescales.

Non-linear concentration-discharge relationships have been widely acknowledged for many contaminants, with assessment of this hysteresis being used as a means of interpreting probable pollutant pathways and origins (e.g. Lefrançois et al., 2007; Naden, 2010; Outram et al., 2014; Smith and Dragovich, 2009). Small scale experiments, in which the pollutant transport processes are controlled, have successfully produced the expected hysteresis dynamics, offering support for this indirect approach (e.g. Chanat et al., 2002; Eder et al., 2014). Analysis of the process dynamics of multiple contaminants using this hysteresis framework enables commonalities in transport systems to be assessed, and maximum information to be extracted about pollutant and catchment response to hydrological events (e.g. Halliday et al., 2014; Mellander et al., 2012; Outram et al., 2014; Owen et al., 2012; Wade et al., 2012). Specifically, this framework enables an assessment of the complicating factors and influences on SS and P transfer at multiple scales (e.g. Haygarth et al., 2012); and, the interaction between catchment structure, connectivity, and pathway dominance under varying environmental conditions (Bilotta et al., 2007; Bilotta et al., 2010; Bracken et al., 2014) .

Such information is valuable and necessary to inform mitigation strategies for reducing diffuse water pollution from agriculture (DWPA) in the UK (McGonigle et al., 2014). The development of a solid evidence base prior to the implementation of mitigation measures is required to: a) determine the effectiveness of control measures (e.g. Wilkinson et al., 2013); b) assess the cost-effectiveness of resource allocation (e.g. Posthumus et al., 2013); and c) enable reliable and transparent decisions to be made about future catchment operations (Collins et al., 2012).

In this present study, high resolution hydro-meteorological, SS and P data collected during a range of low and moderate magnitude runoff events over one year are analysed to determine the intra-storm hysteresis dynamics of SS, TP and TRP concentrations. Analysis of the environmental factors associated with observed pollutant dynamics is conducted using Factor Analysis (FA) which incorporates a suite of environmental variables representing the event storm conditions and antecedent hydro-meteorological conditions. The aim of this analysis is to extract fundamental information describing the transport pathways and pollutant dynamics of the system, providing the basis for examining the key components driving the transfer of SS and P at multiple scales across a small agricultural catchment in the UK.

2   Materials and Methods

2.1   Study Area

This research was conducted in the upper reaches of the Newby Beck sub-catchment of the River Eden, NW England, UK (Figure 1). Newby Beck is a predominantly upland catchment with moderate slopes (7.4%) and a mean elevation of 234 m. The catchment is underlain by steeply dipping, fractured limestone and sandstone units with interbedded siliciclastic argillaceous rock of the Carboniferous period. The soils draining the headwaters in the south of the catchment are well drained, locally deep, fine loamy soils with slowly permeable and seasonally wet acid loamy and clayey soils through the middle reaches, moving towards slowly permeable, seasonally waterlogged reddish fine and coarse loamy soils in the north of the catchment (Cranfield University, 2014). The catchment was designated as a priority under the England Catchment Sensitive Farming Delivery Initiative (ECSFDI) to reduce diffuse water pollution resulting from farming activity. Improved grassland dominates the catchment (76% by area), along with acid grassland (10%) and arable land (6%), with 2.88 livestock units (LU) ha^{-1} (cattle and sheep). The average Olsen P concentration from across 38 fields (14% of catchment) is 23.6 mg kg^{-1} (σ = 9.9 mg kg^{-1}) with a range of 8 – 46 mg kg^{-1}. The

climate of this region is cool temperate maritime with a long-term average rainfall of 1187 mm (σ = 184 mm) (Met Office, 2009). The catchment responds relatively rapidly with a time-to-peak of 3 h (Houghton-Carr, 1999) and the standard percentage runoff (SPR) is estimated to be 35% based on the Hydrology of Soil Types (HOST) classification.
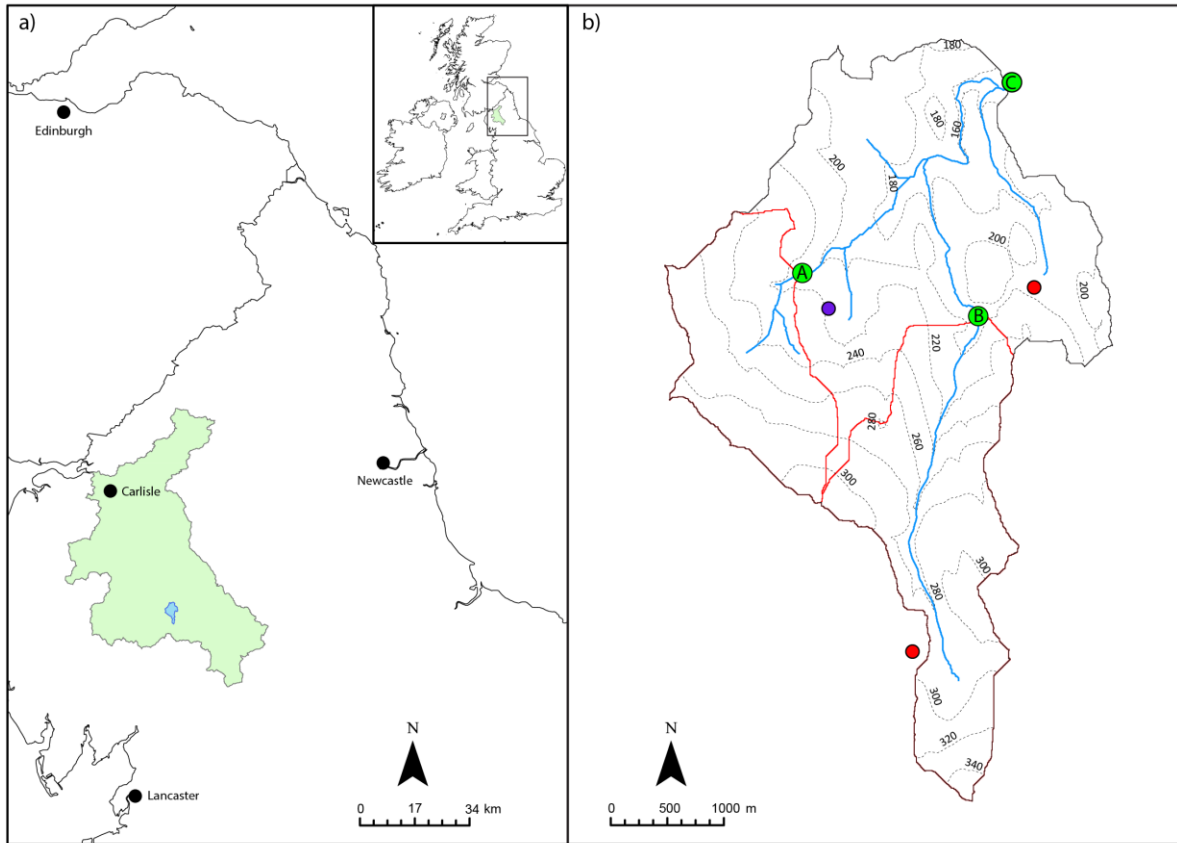

Figure 1: a) Regional map showing the location of the Eden and Newby Beck catchments, coloured green and blue respectively. **b)** Detailed map of the Newby Beck catchment. Locations of rain gauges are represented by red points, the weather station is coloured purple and in-stream water quality stations are coloured green. Contour intervals are 20m. © Crown Copyright/database right 2014. An Ordnance Survey/EDINA supplied service.

2.2 Research Design

This study utilises the River Eden Demonstration Test Catchment (DTC) research platform (cf. Owen et al., 2012). The DTC programme was implemented to inform policy and practical approaches for the reduction of DWPA and the improvement of ecological status in freshwaters, whilst maintaining economically viable food production (McGonigle et al., 2014). The Newby Beck catchment consists of three hydro-meteorological monitoring stations distributed across the catchment (Table 1), with in-stream monitoring stations located

6

at strategic points to effectively partition the catchment into two sub-catchments: (A) 2.2 km^2, and (B) 3.8 km^2, with the outlet monitoring station (C) draining an area of 12.5 km^2.

	Sub-catchment A	Sub-catchment B	Outlet (C)
Monitoring Location (WGS 1984)	54°34'13.5"N	54°34'00.2"N	54°35'07.3"N
	2°38'54.2"W	2°37'29.0"W	2°37'12.2"W
Catchment Area (km^2)	2.2	3.8	12.5
Mean Elevation (m AOD)	261.03	275.49	234.22
Catchment Average Slope (m m^{-1})	0.0600	0.0825	0.0746
Geology (as % of area)			
Limestone	51.43	54.15	50.80
Limestone + shales	48.47	45.85	49.00
Sandstone + shales	0.00	0.00	0.20
Soil Drainage (as % of area)			
Well drained	25.47	69.02	20.12
Seasonally wet	74.53	30.98	65.69
Seasonally waterlogged	0.00	0.00	14.19
Major Land-use Units (as % of area)			
Improved Grassland	65.35	82.89	76.42
Acid Grassland	17.88	12.53	9.84
Arable	9.66	1.25	6.16
Woodland	4.69	2.70	2.36
Other	2.42	0.63	5.22
Average Olsen P (mg Kg^{-1})	---	---	23.6
Standard Percent Runoff (%)	---	---	35
Time to peak (Hours)	---	---	3

Table 1: Description of the characteristics for each of the monitored sub-catchments of the Newby Beck catchment.

2.3 Instrumentation and Sampling

2.3.1 Hydrometeorology

The catchment was equipped with an Environmental Measurement Limited (EML) Automatic Weather Station (AWS), logging rainfall (mm), air temperature (ºC) and net radiation (W m^{-2}) every 15 min. Two additional Casella 0.2 mm tipping bucket rain gauges log on an event basis (Figure 1). Each in-stream monitoring station was equipped with a non-vented SWS Mini-Diver, which when corrected for atmospheric pressure, record water level

(± 0.005 m; i.e. < 0.5% of maximum gauged level) at 5 minute intervals. Site specific rating-curves were produced using river level data and the collection of flow measurements. Velocity measurements were taken using a Valeport Electromagnetic Current Meter at low flows and a Teledyne RD Instruments StreamPro ADCP during high-flows. Discharge values were calculated using the Area-Velocity method. At peak flows, extrapolation of the rating curves beyond the maximum gauged discharge was necessary for 2.96, 0.67 and 0.61% of the time for Stations A, B and C, respectively. This was achieved using the Velocity Area Rating Extension (VARE) approach (Ewen et al., 2010).

2.3.2   Water Quality Parameters

Turbidity probes were deployed at all three in-stream monitoring stations to provide high-frequency surrogate measurements of suspended sediment concentrations. Measurements were made at fifteen minute intervals using McVan Analite 395 nephelometers (Stations A and B) and a YSI 6600 multi-parameter sonde (Station C). These probes were equipped with wipers, programmed to clean the sensor at sub-hourly intervals. At Station C, P concentrations were measured using a Hach Lange combined Sigmatax sampling module and Phosphax Sigma analyser. The system was subjected to a weekly cleaning cycle, with automatic calibration with a 2 mg L^{-1} standard solution being performed daily. TP is determined colourimetrically following heating of the sample to 140ºC under pressure and being subjected to persulfate digestion, whilst molybdate-reactive phosphorus (TRP) concentrations are determined colourimetrically on an unfiltered sample (Elisenreich et al., 1975; Wade et al., 2012). TRP is an operationally defined measurement predominantly comprised of orthophosphate (PO_4; SRP), although readily hydrolysable P species in the sample may also be present within this TRP fraction (Halliday et al., 2014). TP and TRP measurements were made alternately every 15 min.

2.4   Quality Control & Data Treatment

2.4.1   Hydrometeorology

Data from the three rain gauges across the catchment were visually compared to detect events that were not registered by individual stations due to malfunction. Following assurance of the data's quality, precipitation from the available stations was interpolated using an Inverse Distance Weighting function (Ahrens, 2006). River level was visually inspected for artificial anomalies. For short-lived erroneous events, anomalies were removed through linear interpolation of adjacent values (cf. Horsburgh et al., 2010).

2.4.2   Water Quality

The limits of detection of the Hach Lange Sigmatax/Phosphax systems were assessed by analysing replicate blank samples consisting of deionised water. These 'blanks' were pumped through the entire system and analysed by the Phosphax analyser. Average concentrations of 0.009 mg L^{-1} for TRP and 0.02 mg L^{-1} for TP were observed. These concentrations were assigned as the limits of detection for the method, with measurements below these values being removed from the dataset. *In-situ* measurements of turbidity, TP and TRP were regularly compared with laboratory derived reference measurements (as defined in Table 2). River samples were obtained for these tests using an ISCO 3700 automatic sampler. Suspended sediment concentration (SSC) was determined using the gravimetric method (American Society for Testing and Materials, 2000). SRP and TP concentrations were analysed by a Konelab Discrete and a Skalar Continuous Flow analyser respectively at the UKAS accredited National Laboratory Service. This laboratory follows standard methodology and both instruments have a limit of detection of 0.001 mg L^{-1}. Preparation of the sample for SRP analysis involved passing the sample through a 0.45 µm cellulose acetate membrane filter to remove solids.

	Turbidity *versus* SSC	*In-situ* TP *versus* Lab TP	*In-situ* TRP *versus* Lab SRP
Station A	X		
Station B	X		
Station C	X	X	X

Table 2: Comparisons made between the *in-situ* measurements and the laboratory derived reference samples for each monitoring station. X indicates a test between the two parameters was conducted.

A linear regression model was adopted to best describe the fit between the *in-situ* and reference measurements for all determinants. A condition specifically imposed for the turbidity-SSC model was that the intercept had to pass through the origin. This was chosen to prevent negative prediction of SSC values at very low turbidity levels (Perks et al., 2014). For each of the developed linear models, the uncertainty of the regression coefficients was evaluated by bootstrapping the residuals 10,000 times, replacing the original sample and providing detailed information about the characteristics of the population.

2.5   *Event Classification and Extraction*

The initiation of a hydrologically significant event was defined following partitioning of the hydrograph into base and storm flow components based on the Hydrograph separation program (HYSEP) local minimum method (Sloto and Crouse, 1996). Initial classification of events was undertaken at the outlet, Station C. Only high flows that were observed at both the sub-catchments were selected for analysis. This resulted in a total of 55 events being retained, which occurred between the 10th of May 2012 and the 14th of February 2013 (Figure 2). At each site, and for events with available data, an assessment of the TP/TRP/SSC hysteresis dynamics was conducted based on the comprehensive account of hysteresis patterns provided by Williams (1989).
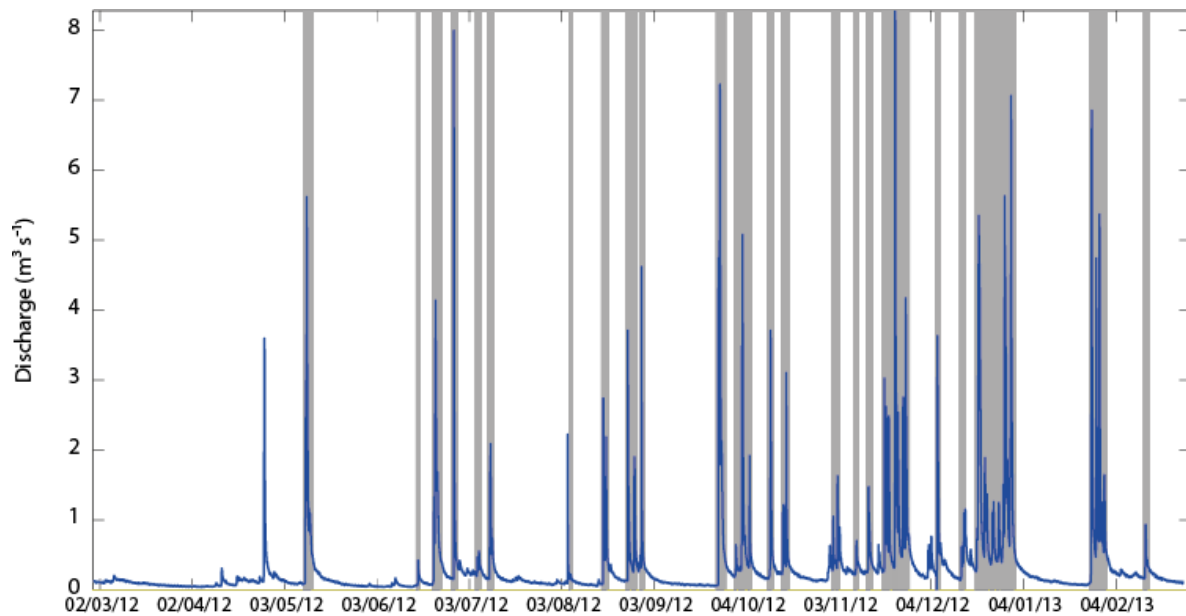

Figure 2: Discharge data generated from during the monitoring period (March 2012 to March 2013) at the catchment outlet (Station C). Hydrologically significant events selected for analysis with suspended sediment and phosphorus data available are highlighted.

2.6   *Factor Analysis*

The compilation of hydrochemistry and meteorology for periods immediately prior to and during the storm events, collected across three water quality and three meteorology monitoring stations, resulted in the production of a complex, multi-dimensional dataset, parameters, units and measurement intervals of which are provided in Table 3. Multivariate statistical treatment of the data was used to extract the underlying information (Singh et al., 2004). Factor Analysis (FA) was chosen to provide a structured and transparent method of analysing the complex dataset. To examine the suitability of the data for FA, the Kaiser–Meyer–Olkin (KMO) and Bartlett's sphericity tests were performed. Following calculation of the KMO measure of sampling adequacy (MSA), individual variables with unacceptable MSA values (< 0.60) were removed following the recommendations of Kaiser (1974). Bartlett's test of sphericity on each of the three z-scale transformed experimental datasets produced a significance level of zero, indicating significant relationships amongst variables. This indicates an adequate degree of common variance, indicating that the matrixes are factorable (Shrestha and Kazama, 2007). A Varimax rotation scheme was employed and a three-factor model determined (Kaiser, 1958).

Variables	Description	Units
Antecedent Conditions		
P1d	Precipitation total for 1 day prior to the event	mm
P5d	Precipitation total for the 5 days prior to the event	mm
P7d	Precipitation total for the 7 days prior to the event	mm
P21d	Precipitation total for the 21 days prior to the event	mm
Q1d	Median discharge for the 1 day prior to the event	$m^3\,s^{-1}$
Q5d	Median discharge for the 5 days prior to the event	$m^3\,s^{-1}$
Q7d	Median discharge for the 7 days prior to the event	$m^3\,s^{-1}$
Q21d	Median discharge for the 21 days prior to the event	$m^3\,s^{-1}$
Qb	Base-flow discharge immediately before the event	$m^3\,s^{-1}$
T1d	Median air temperature for 1 day prior to the event	°C
T5d	Median air temperature for 5 days prior to the event	°C
T7d	Median air temperature for 7 days prior to the event	°C
T21d	Median air temperature for 21 days prior to the event	°C
Event Hydrology		
Pt	Event precipitation total	mm
IMax	Maximum precipitation intensity	mm 15 min^{-1}
Q max	Maximum event discharge	$m^3\,s^{-1}$
Q mean	Mean event discharge	$m^3\,s^{-1}$
QR max	Maximum rise in discharge	m^3
QR mean	Mean rise in discharge	m^3
Wt	Water yield	hm^3
Soluble and Particulate Transport		
SSC max	Maximum suspended sediment concentration	mg L^{-1}
SSC median	Median suspended sediment concentration	mg L^{-1}
Sediment flux	Suspended sediment flux	tonnes
TP flux	Total phosphorus flux	kg
TP max	Maximum Total Phosphorus concentration	mg L^{-1}
TP median	Median Total Phosphorus concentration	mg L^{-1}
TRP flux	Total Reactive Phosphorus flux	kg
TRP max	Maximum Total Reactive Phosphorus concentration	mg L^{-1}
TRP median	Median Total Reactive Phosphorus concentration	mg L^{-1}

Table 3: Abbreviations, names and units for the variables entered into the factor analysis

3 Results

3.1 Performance of In-Situ and Surrogate Measurements

The performance metrics of each of the *in-situ* (TRP/TP) and surrogate (turbidity) measurements used in this study are provided in Table 4. These include the uncertainty of the regression coefficients for each developed model, along with the number of calibration samples (*n*) and summary statistics. It is demonstrated that turbidity is an excellent surrogate for SSC, with each of the developed linear models being highly statistically significant ($P <$ 0.001). These site specific models were used for calibration, with turbidity being converted to SSC. The relationship between the *in-situ* and laboratory derived TP concentrations is also highly significant (R^2 = 0.97; $P <$ 0.001) although the field measurements typically overestimate the reference (laboratory derived) concentrations. This is likely an artefact of different analytical procedures and the reagents used during the *in-situ* analysis. However, this does provide assurance that the Hach Lange apparatus is operating in a stable and precise manner. An additional comparison was made between the *in-situ* TRP and lab-based orthophosphate (SRP) concentrations. Although these are essentially different determinands, a relationship between the two may be expected given that TRP includes SRP plus any easily hydrolysable P species. Linear regression between the two results in a statistically significant relationship (R^2 = 0.80; $P <$ 0.001), with the field measurements of TRP exceeding orthophosphate concentration as expected. Interpretation of the model coefficients suggests that the vast majority of TRP found within this headwater catchment is of soluble reactive form (Table 4).

	Regression Equation (y = ax *or* y = a + bx)	Range (mg L^{-1})	a [95% CI]	*b* [95% CI]	R^2
Station A					
Turbidity *versus* SSC (*n* = 76)	y = 1.5386x	4.9 – 815.0	1.448 – 1.629	---	*0.92*
Station B					
Turbidity *versus* SSC (*n* = 89)	y = 1.1645x	3.0 – 778.0	0.991 – 1.254	---	*0.72*
Station C					
Turbidity *versus* SSC (*n* = 108)	y = 1.5655x	3.0 – 386.0	1.418 – 1.625	---	*0.83*
In-situ TP *versus* Lab TP (*n* = 128)	y = -0.0103 + 0.8649x	0.02 – 0.51	-0.017 – -0.004	0.838 – 0.89	*0.97*
In-situ TRP *versus* Lab SRP (*n* = 129)	y = -0.0055 + 0.8629x	0.07 – 0.20	-0.013 – 0.002	0.783 – 0.934	*0.80*

Table 4: Summary statistics of field calibrations for measurements made by turbidity probes and Phosphax analyser. Confidence intervals (CI) of the model coefficients (a and *b*) are

provided following bootstrapping of the residuals, where $n = 10,000$. Relationships that are significant at the 99.9% level are italicised.

3.2   *Factor Analysis*

Taking samples and variables into account, three factors explained 82.75%, 72.61%, and 74.71% of the variance for monitoring stations A, B and C, respectively. In order to determine the dominant variables of each factor, loadings were computed. 'Strong', 'moderate' and 'weak' loadings are defined as > 0.75, $0.75 - 0.50$ and $0.50 - 0.30$, respectively (Shrestha and Kazama, 2007). For each of the stations, the factor which explains the greatest variance in the dataset (i.e., factor one) is characterised by high positive factor loadings (> 0.75) for the event storm conditions. These include variables such as the mean and maximum discharge, rate of discharge rise, precipitation total and the mass of suspended sediment transported during the event (Table 5). Factor two is characterised by high positive factor loadings for variables describing the antecedent hydrological conditions prior to the commencement of the storm event. These include the amount of precipitation over the preceding 1/5/7/21 days and the discharge associated with these antecedent periods. The third factor is characterised by high positive factor loadings for variables describing the ambient temperature over the preceding 1/5/7/21 days. These three factors which were retained for Varimax rotational analysis and utilised to understand the necessary conditions for the production of distinct hysteresis loops therefore represent: 1) event magnitude; 2) antecedent wetness; and 3) temperature.

Variables	Factor loadings for Station A			Factor loadings for Station B			Factor loadings for Station C		
	Factor 1	**Factor 2**	**Factor 3**	**Factor 1**	**Factor 2**	**Factor 3**	**Factor 1**	**Factor 2**	**Factor 3**
P1d					0.58			0.59	
P5d		**0.92**			**0.91**			**0.92**	
P7d		**0.94**			**0.87**			**0.87**	
Q1d		0.58			0.64			0.71	
Q5d		**0.99**			**0.91**			**0.93**	
Q7d		**0.99**			**0.90**			**0.90**	
Q21d		0.57							
Qb								0.56	
Pt	0.71						**0.82**		
Q max	**0.97**			**1.00**			**0.96**		
Qmean				**0.83**			**0.82**		
QR max	**0.82**			**0.88**			0.73		
QR mean	**0.88**			**0.92**			**0.87**		
SSC max	0.74			0.68			**0.87**		
IMax	0.74						0.72		
Wt				0.64					
Sediment flux	**0.95**			**0.93**			**0.95**		
TP Flux							**0.86**		
TRP max							0.56		
TRP median									
T1d			**0.94**			**0.91**			**0.90**
T5d			**0.99**			**0.99**			**0.93**
T7d			**0.99**			**0.99**			**0.98**
T21d			**0.94**			**0.93**			**0.99**
Explained Variance (%)	39.62	23.23	19.90	30.18	25.03	17.40	34.80	25.42	14.48
Cumulative Explained Variance (%)	39.62	62.85	82.75	30.18	55.21	72.61	34.80	60.23	74.71

Table 5: Summary of factor loadings for all variables accepted for use in FA for Newby Beck monitoring stations A, B and C. Only factor loadings ⩾ 0.5 are provided with values ⩾ 0.75 presented in bold.

3.3   Suspended Sediment

At monitoring station A, hysteresis patterns are almost entirely dominated by clockwise hysteresis (86.2%; Figure 3a). These events are the dominant behaviour of the system and occur across the full range of factor conditions, represented by the large standard deviation (σ) of factor (F) scores (s) (F1 $\bar{s} = 0.11$, $\sigma = 1.03$; F2 $\bar{s} = 0.10$, $\sigma = 1.04$; F3 $\bar{s} = -0.15$, $\sigma = 0.99$). For 10.4% of events, figure-of-eight with an anti-clockwise loop (A8) hysteresis is observed.

These events are characterised by negative factor one and factor two scores (F1 $\bar{s}$ = -0.55, σ = 0.51; F2 $\bar{s}$ = -0.53, σ = 0.37), and high factor three scores (F3 $\bar{s}$ = 0.89, σ = 0.38), demonstrating their predisposition to occur following warm, dry periods during low magnitude events. Anti-clockwise events are also observed (3.4% of events) under similar conditions to that of A8 events (F1 $\bar{s}$ = -1.20, F2 $\bar{s}$ = -0.79; F3 $\bar{s}$ = 1.29).

At monitoring station B, within-storm sediment dynamics are again dominated by clockwise hysteresis (86.8%; Figure 3b), occurring across the full range of factor score conditions (F1 $\bar{s}$ = 0.10, σ = 1.04; F2 $\bar{s}$ = 0.01, σ = 1.01; F3 $\bar{s}$ = -0.16, σ = 0.96). A8 events are again found to occur infrequently (9.4%). These occur under similar conditions to those observed at monitoring station A; i.e. low factor one scores (F1 $\bar{s}$ = -0.71, σ = 0.24), low factor two scores (F2 $\bar{s}$ = -0.66, σ = 0.29) and high factor three scores (F3 $\bar{s}$ = 1.26, σ = 0.41). The remaining events (3.8%) are described as having no discernible hysteresis pattern and are characterised as having low factor one scores (F1 $\bar{s}$ = -0.51, σ = 0.16), high factor two scores (F2 $\bar{s}$ = 1.46, σ = 1.03) and high factor three scores (F3 $\bar{s}$ = 0.61, σ = 0.29).

At monitoring station C, hysteresis patterns are varied despite clockwise hysteresis events being most prominent (Figure 3c). 42.2% of events can be described as exhibiting clockwise hysteresis, which occurs across the spectrum of factor score conditions (F1 $\bar{s}$ = 0.59, σ = 1.10; F2 $\bar{s}$ = 0.04, σ = 1.01; F3 $\bar{s}$ = -0.14, σ = 0.98). Both A8 and anti-clockwise events also occur in significant numbers at the outlet station, contributing to 20% and 22.2% of the total, respectively. Similarly to monitoring stations A and B, A8 events occur when factor one scores are negative ($\bar{s}$ = -0.25, σ = 0.45) i.e. during low-moderate magnitude events. However, these are also characterised by high factor three and low factor two scores, or the inverse (F2 $\bar{s}$ = 0.54, σ = 0.92; F3 $\bar{s}$ = 0.29 σ = 0.94). Anti-clockwise events predominately occur during events characterised as having highly negative factor one and factor two scores (F1 $\bar{s}$ = -0.75, σ = 0.19; F2 $\bar{s}$ = -0.64, σ = 0.70). The remaining events may be characterised as exhibiting figure-of-eight with a clockwise loop (C8) hysteresis (4.4%) and no discernible hysteresis pattern (11.1%).

3.4 Total Reactive Phosphorus

At monitoring station C, the within-storm dynamics associated with TRP are dominated by anti-clockwise hysteresis (62.2%; Figure 3d). These events occur across the full range of varifactor conditions with the exception of events that are characterised by a combination of high VF1 and VF2 conditions (VF1 $\bar{s}$ = -0.20, σ = 0.66; VF2 $\bar{s}$ = -0.02, σ = 0.99; VF3 $\bar{s}$ = -0.13, σ = 1.01). C8 events are also frequently observed (17.8%) and these events are characterised by high VF1 scores, although they do occur across the full range of VF conditions (VF1 $\bar{s}$ = 0.68, σ = 1.42; VF2 $\bar{s}$ = 0.17, σ = 1.07; VF3 $\bar{s}$ = 0.19, σ = 0.90). The remaining events are characterised as exhibiting clockwise (6.7%) or no discernible hysteresis (13.3%).

3.5 Total Phosphorus

At monitoring station C, the within-storm dynamics associated with TP are almost entirely dominated by anti-clockwise hysteresis (73.3%; Figure 3e). This is the dominant behaviour of the system and occurs across the full range of varifactor conditions with the exception of events which are characterised by a combination of high VF1 scores and negative VF3 scores (VF1 $\bar{s}$ = -0.18, σ = 0.80; VF2 $\bar{s}$ = 0. 14, σ = 0.99; VF3 $\bar{s}$ = -0.01, σ = 1.03). C8 type events account for a further 13.3%, which are also not limited to specific conditions, although they do dominate when VF1 is high ($\bar{s}$ = 0.80, σ = 1.19) and when VF3 is low ($\bar{s}$ = -0.26, σ = 0.53) i.e. moderate-high magnitude events in periods of low ambient temperature. Remaining events may be characterised as exhibiting A8 (4.4%), clockwise (2.2%), and no discernible hysteresis (6.7%).
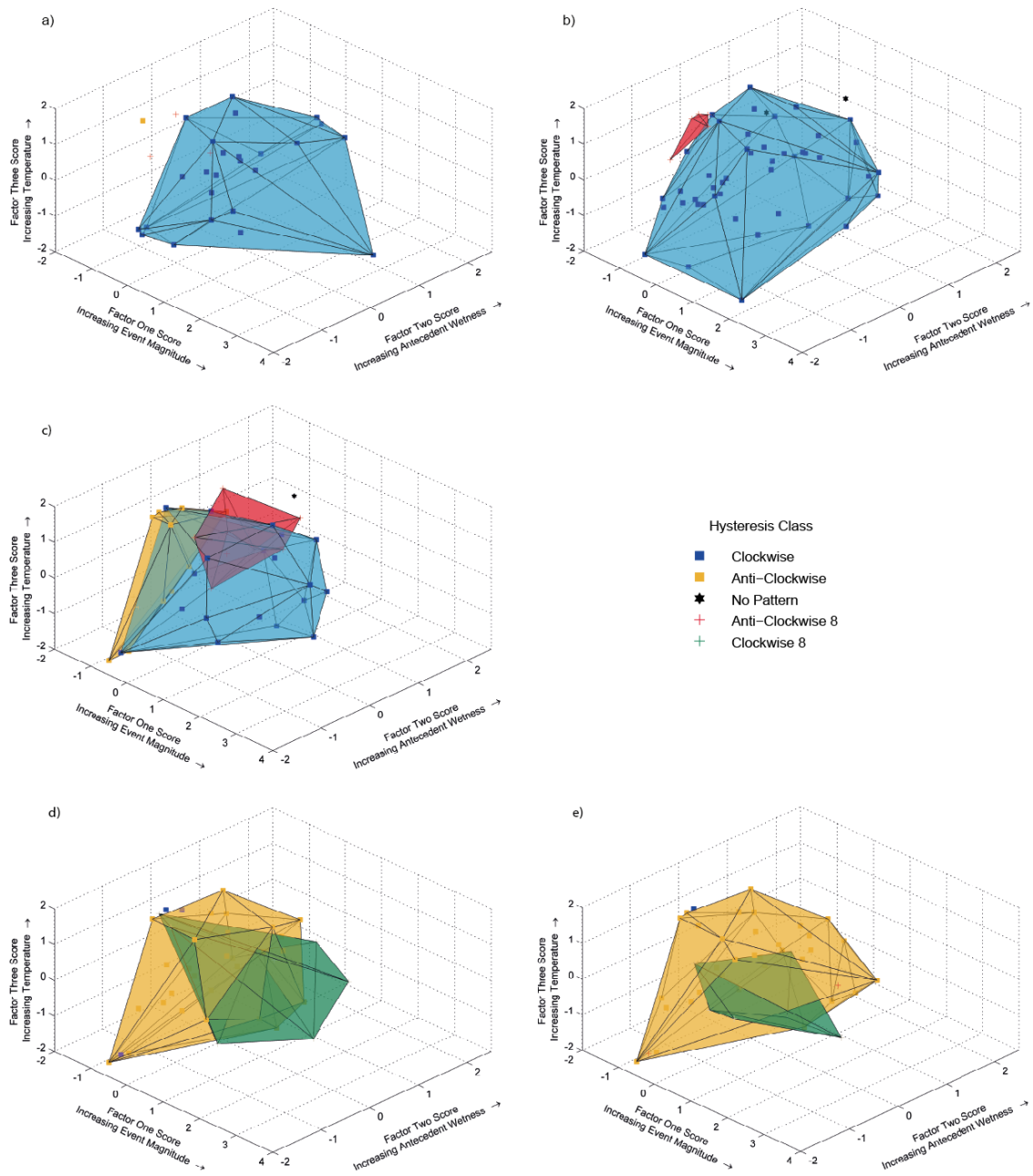
Figure 3: Distribution of events in the I-III factorial plane according to hysteresis classification for **a)** suspended sediment at station A (*n* = 29); **b)** suspended sediment at station B (*n* = 53); **c)** suspended sediment at station C (*n* = 45); **d)** total reactive phosphorus at station C (*n* = 42); and **e)** total phosphorus at station C (*n* = 45).

4   Discussion

4.1   Suspended Sediment Transfer in Response to Temporal and Spatial Constraints

Clockwise hysteresis events dominate, accounting for 86% and 89% of events and for 96% and 99% of the sediment flux generated during storm periods at Stations A and B, respectively. The incidence of these events is consistent between sub-catchments, with comparable hysteresis responses occurring on 93% of occasions. The rapid response of SSC to hydrological forcing implies that the SS sources are readily accessible with the majority of SS being generated from areas proximal to the channel (Bača, 2008; Lefrançois et al., 2007; Rodríguez-Blanco et al., 2010). These sediment sources include: bed material (Arnborg et al., 1967; Bogen, 1980), bank material (Langlois et al., 2005; Seeger et al., 2004; Smith and Dragovich, 2009) and hydrologically connected areas close to the channel which respond rapidly at the onset of a storm (Mano et al., 2009; Reid et al., 2007). Factor analysis has illustrated that these event dynamics have no threshold of initiation and may occur across the full range of environmental conditions observed.

A secondary response at the sub-catchment scale, which is infrequently observed, is figure-of-eight hysteresis with an anti-clockwise loop (A8). This is a result of temporary elevated SSCs on the rising limb, followed by a period of enhanced transfer following peak discharge. The processes producing A8 events are difficult to decipher, although the enhanced SSC at low discharges on the rising limb of the hydrograph is likely a result of event water prominence and more specifically, within-channel sediment sources that are readily mobilised during the initial stages of the event (Eder et al., 2014). Such event characteristics are likely a result of rapid remobilisation of material deposited during the recession period of the previous event (Bull, 1997; Eder et al., 2014). Factor analysis has indicated that the occurrence of these events at Stations A and B is preceded by a combination of fluvial quiescence and relatively high air temperatures. These antecedent hydro-meteorological characteristics will be a principal control of the preparatory processes operating during the relaxation period between events, and they may govern the rate of sediment generation and condition the system response (Bracken et al., 2014; Lexartza-Artza and Wainwright, 2009). For example, an extended recession period may result in the relative abundance of easily accessible within-channel sources being present due to a lack of depletive flows (Carling, 1983; Stutter et al., 2008; VanSickle and Beschta, 1983). Meanwhile, elevated temperatures and high net radiation would enhance the presence of in-stream vegetation producing a

stabilising effect and efficiently trapping fine grained material within the channel at base-flow (Cotton et al., 2006). These characteristics may act to increase the within-channel availability of fine sediment throughout the relaxation period, with the subsequent storm mobilising this accumulated and easily accessible sediment stock, triggering the initial elevated SSCs; the initial phase of the A8 hysteresis pattern. The continued transfer of sediment through the system on the falling limb of the hydrograph is however indicative of a delayed contribution from an additional significant sediment source (Eder et al., 2010).

At the catchment scale (Station C), clockwise hysteresis is still highly important in the export of SS from the Newby Beck catchment. Despite accounting for only 42% of events, they account for 75% of total flux generated during storms. Events classified as clockwise at Stations A and B are, however, only replicated at the outlet on 47% and 56% of occasions respectively, with an increased incidence of A8 and anti-clockwise hysteresis at this catchment-scale. This lack of uniformity between sub-catchments and the catchment outlet reflects between-scale variations in dominant processes and may reflect inconsistencies in sediment sources (Smith and Dragovich, 2009). An example of the between scale divergent response is provided in Figure 4. In this instance, a storm producing 11.8mm of rainfall results in a catchment-wide hydrological response and the creation of broad, clockwise SS hysteresis loops at both Stations A and B. However, at Station C, these dynamics are not replicated, and an A8 loop is produced. This is a commonly observed variant response throughout the time-series, representing 20% of events at the outlet and producing 9% of the storm generated flux. Similar to Stations A and B, these events occur during low-moderate magnitude run-off events with their occurrence across a gradient of antecedent conditions and ambient temperature (Figure 3c).
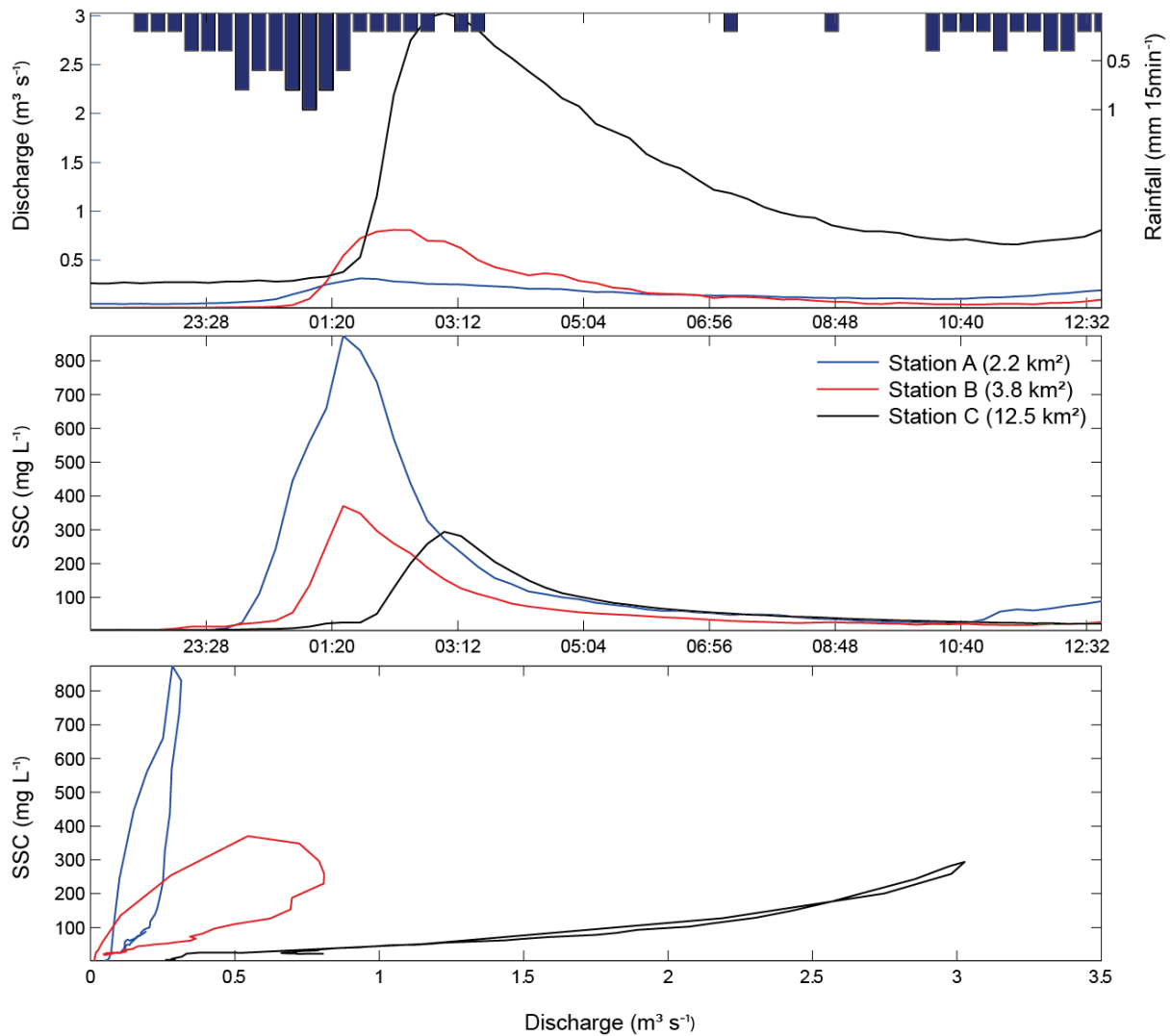
Figure 4: An example of the divergent suspended sediment hysteresis dynamics with increasing scale over the course of a catchment-wide storm beginning on the 18th November 2012.

More striking inconsistencies in the SS hysteresis patterns between scales are observed when the occurrence of anti-clockwise hysteresis is examined. These event dynamics are extremely infrequently reported at Stations A and B. However, at Station C these account for 22% of the events, and 2% of the storm generated sediment flux. The generation of these sediment dynamics is likely the result of the dominant sediment delivery pathway being a) extensive with a source distal to the main channel (Eder et al., 2010; Marttila and Kløve, 2010), or b) slow-moving (Sadeghi et al., 2008). Given that these dynamics are observed at the outlet station only, during low magnitude events and following relatively dry antecedent conditions, it is highly unlikely that contributing area expansion, the capturing of headwater zones and widespread hydrological connectivity would result in significant contributions from distal

sources (Bača, 2008; Giménez et al., 2012; Marttila and Kløve, 2010; Webb and Walling, 1982). Rather, given the event characteristics, sub-surface flow is anticipated to be a significant contributor to both the storm-water discharge and, potentially, the material flux (e.g. Deasy et al., 2009; Russell et al., 2001). Sub-surface particulate fluxes are likely to occur following soil pipe erosion (Verachtert et al., 2011), or detachment at the surface by raindrop impact which is subsequently delivered through soil macro-pores or sub-surface drains (Pilgrim and Huff, 1983). Although these sub-surface processes may be important during low magnitude events, as storm intensity increases, additional pathways of sediment movement become progressively important (Sayer et al., 2006), limiting the occurrence of anti-clockwise hysteresis events to low magnitude runoff events.

These findings highlight the importance of spatial constraints on controlling the dynamics of sediment transfer. As scale increases, SS transmission is complicated by the dominance and variability of erosive processes and connected pathways in the catchment (de Vente and Poesen, 2005; Lexartza-Artza and Wainwright, 2011). In Newby Beck, this spatial dependency is likely a consequence of the transition from the relatively freely draining soils of the elevated sub-catchments to the lower-lying, slowly permeable soils of the wider catchment, which necessitates the increased presence of under-drainage for sustainable agricultural production (cf. Table 1). The manifestation of this is a small reduction in surface driven sediment transfer at the catchment scale, and conversely, a greater incidence of slow-moving pathways, as a result of disconnection between the surface supply – delivery system. Furthermore, although surface pathways dominate in terms of SS delivery at each spatial scale, there is a temporal dependency that influences the dominance of a particular pathway, especially at increasing spatial scales where catchment linkages become more complex. It is clear that key environmental drivers alter the distribution of pollutant pathways, with delivery of SS through shallow sub-surface pathways during low magnitude events becoming increasingly frequent despite transferring relatively little in terms of total flux.

4.2   *Dominant Pathways of Phosphorus Transfer*

Monitoring of TRP and TP at Newby Beck has provided new insights into the processes responsible for their delivery in a headwater agricultural catchment. In catchments dominated by 'natural sources', P is mobilised by physical processes of erosion, with the majority of transfer typically taking place in particulate form (Jarvie et al., 2008; Withers and Jarvie, 2008). In Newby Beck, this particulate contribution is secondary to the predominantly soluble

TRP fraction, with a median event ratio between TRP and TP of 0.57:1. This suggests the importance of anthropogenically derived sources, with excess fertiliser application possibly leading to a potential surplus of nutrient stock that is not exhausted (Römer, 2009).

This analysis has revealed that the dominant pathways of P delivery to the fluvial system are largely distinct to the pathways responsible for delivering SS, with anti-clockwise hysteresis dominating both the TRP and TP time-series of events (Figure 3). Previous studies have inferred these dynamics to be a consequence of point sources such as septic tanks and dairy shed retention ponds, which continue to contribute following the hydrograph peak (McKee et al., 2000). However, in this instance, the positive relationship between discharge and P concentrations on a seasonal and event-basis and the lack of dilution-effects does not support this interpretation (Jarvie et al., 2008). Rather, the dominance of anti-clockwise hysteresis provides support for a non-channel source, with soil water being the dominant pathway (Bowes et al., 2005; Chanat et al., 2002; Hatch et al., 1999). Although this may not be typical of agricultural catchments (e.g. Harrington and Harrington, 2014; Sharpley et al., 1992; Siwek et al., 2013), near-surface runoff as a conduit for effective P transfer has been highlighted in other headwater catchments, with the presence of field drains producing preferential hydrological pathways (Dils and Heathwaite, 1999; Hatch et al., 1999; Heathwaite et al., 2006; Heathwaite and Dils, 2000; Rhea et al., 1996; Sims et al., 1998). This sub-surface pathway will not only enable the movement of soluble P within the soil matrix, but also very fine colloidal material, which may contribute significantly to the export of TP and TRP (Foster et al., 2003; Heathwaite and Dils, 2000). Given the potential for both particulate and soluble fractions to be effectively transported by these sub-surface connections, a great deal of synchronicity in TP and TRP hysteresis dynamics is observed, with 82% of the events producing anti-clockwise hysteresis for TRP resulting in a comparable TP response (e.g. Figure 5). It is this shallow sub-surface component that is dominant in over 73% of the events analysed for TP and 62% for TRP. These pathways are also responsible for a significant proportion of the event P flux, with anti-clockwise hysteresis events accounting for 49% of the storm driven P flux.
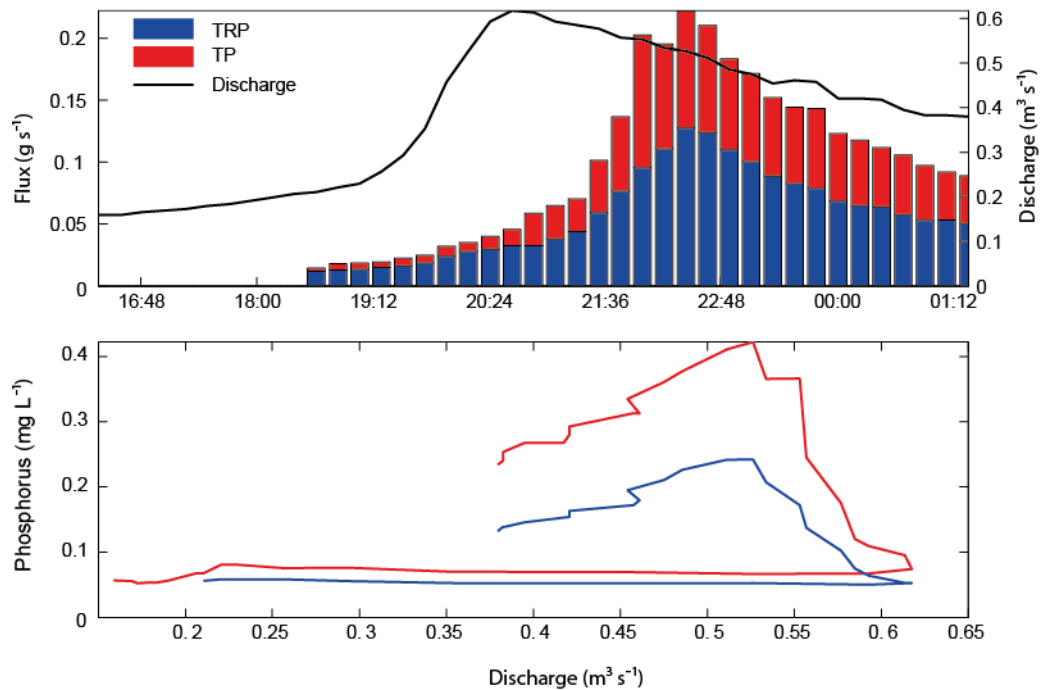
Figure 5: An example of the anti-clockwise hysteresis dynamics exhibited for total phosphorus (TP) and total reactive phosphorus (TRP) at Station C. Figure **5a)** illustrates the delay in both TP and TRP fluxes in the catchment, with TRP becoming less dominant during times of peak flux. Figure **5b)** illustrates the magnitude of anti-clockwise hysteresis observed for TP and TRP concentrations.

The alternate C8 hysteresis dynamics may only account for 13% of events but they represent 25% of the storm driven P flux. The C8 pattern is the result of P concentrations responding moderately at the beginning of the event, prior to a surge in concentrations towards peak discharge on the rising limb of the hydrograph (e.g. Figure 6). These dynamics are mainly observed during moderate and high magnitude events for both TRP and TP. The threshold type behaviour observed during the rising-limb is indicative that the factor(s) constraining the transfer of mobilised particulate material have been overcome. In this instance, usually disconnected depositional zones may become linked to the fluvial networks as a result of intense rainfall across the catchment. In these usually disconnected depositional zones, sediment can be an important source of P (Quinton et al., 2010), which, when activated and connected to the wider catchment can result in the transfer of vast fluxes of P in surface water (cf. Haygarth et al., 1999). Upon rainfall subsiding, concentrations rapidly decline as surface runoff ceases (Siwek et al., 2013), with a secondary pulse being observed on the falling limb of the hydrograph as P enters the river via shallow through-flow pathways.
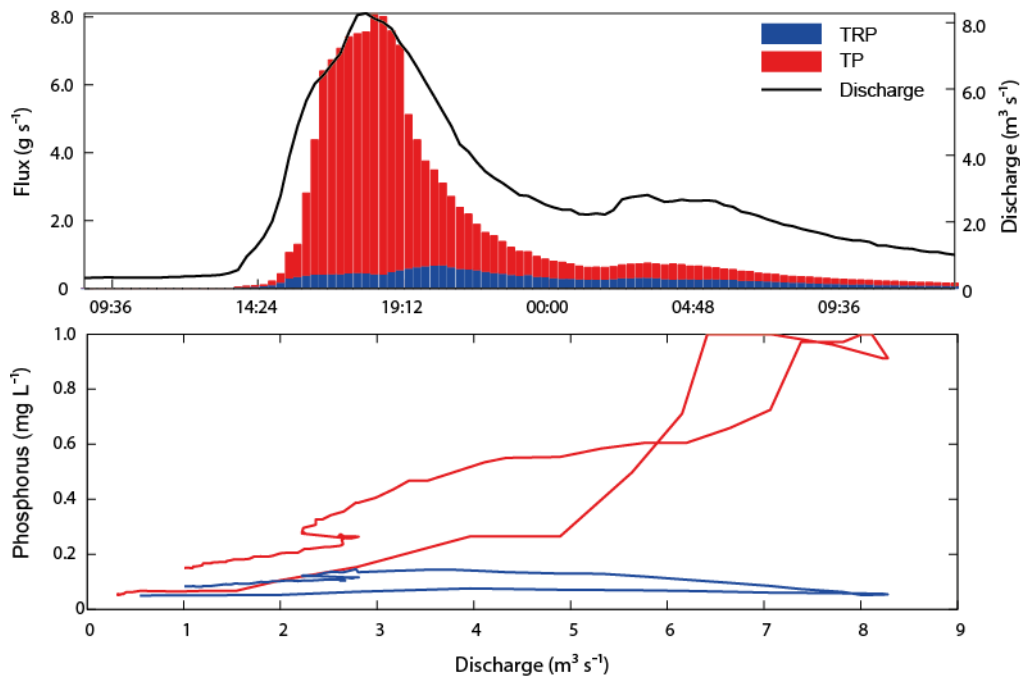
Figure 6: An example of the figure-of-eight (clockwise loop) hysteresis dynamics exhibited for total phosphorus (TP) and total reactive phosphorus (TRP) during infrequent but high magnitude events. Figure **6a)** illustrates the synchronicity of both TP and TRP fluxes in the catchment, with TRP becoming less dominant as runoff increases rapidly. Figure **6b)** illustrates the timing of concentration pulses which lead to the production of the figure-of-eight (clockwise loop) hysteresis.

4.3   Implications for Catchment Management

This analysis provides a behavioural understanding that has important implications for reducing P and fine sediment exports within predominantly grassland headwater catchments, with divergent delivery mechanisms being identified between contaminants and across the catchment-unit. The dominant clockwise hysteresis dynamics for suspended sediment highlights fast, surface-water driven delivery from areas proximal to the channel. In these agricultural catchments, transfer of pollutants as a result of infiltration-excess flow should be rare, however, land management practices commonly used in food production increase compaction and soil degradation, enhancing its occurrence (Heathwaite et al., 2005). Where soil structure is compromised, soil resistance and function could be restored through the use of soil aeration and sward lifters to improve soil infiltration. Where surface runoff pathways are driven by topographic, or man-made features such as tracks and tractor wheelings, physical interception is required to prevent potential sediment source areas becoming CSAs. Decoupling of the hillslope-channel system may be achieved by proactively disconnecting

25

these linkages through the creation of within field, or field edge detention areas through the use of soil bunds, woodland buffer zones, or offline storage ponds. These features slow and temporarily store runoff, enabling mobilised sediment to be recaptured in strategic locations (Burt, 2001; Jordan et al., 2003; Wilkinson et al., 2013). Accessible sediment and P sources from the channel networks could also be further reduced by fencing channels to reduce livestock access. The slow-moving, near surface dominant pathway identified for TP and TRP can only be addressed through a combination of improving soil condition and structure to reduce the occurrence of dry cracked soils and macro-pores; fertiliser management to reduce the source and; proactive interception of land-drains at their outfall within the farm ditch system. The issue of disconnecting depositional zones that become active during infrequent high magnitude events is somewhat more troublesome and requires whole-farm planning and careful nutrient budgeting.

5   Conclusion

Assessment of the intra-event hysteresis dynamics and factor analysis of hydro-chemical and suspended sediment datasets for a small agricultural catchment has provided indirect evidence of the dominant mechanisms and pathways of SS and P transfer. At both the sub-catchment ($2.2 - 3.8$ km^2) and catchment scale (12.5 km^2) and across the complete range of antecedent and hydrological conditions observed, SS is delivered to the fluvial systems predominantly via a rapidly responding pathway close to the drainage network. At the sub-catchment scale, figure-of-eight hysteresis with an anti-clockwise loop is infrequently evidenced; however these are not controlled by the event hydrology, but rather the antecedent conditions and ambient temperature. This highlights the importance of preparatory processes during the relaxation period. SS is also observed to be delivered via a slow moving pathway during 22% of events at the catchment outlet. These are low magnitude events, during which SS is delivered to the fluvial network predominantly via sub-surface pathways. Remarkably, P has been revealed to exhibit a distinct hysteresis response to that of SS. Anti-clockwise hysteresis dominates, accounting for 73% and 62% of events for TP and TRP. This slow moving pathway may be atypical of agricultural catchments, but represents the importance of near-surface runoff as a conduit for P transfer. During high magnitude events however, figure-of-eight hysteresis with a clockwise loop is observed. This threshold-like behaviour is likely the result of the activation and connection of usually disconnected depositional zones to the fluvial networks which results in the transfer of vast P fluxes. The divergent dynamics observed between contaminants across this small agricultural catchment exemplifies the

complexity and variability of fine sediment and P transfer processes, highlighting the need to understand dominant pollutant pathways and for the development of contaminant specific management plans to ensure that control measures are most effective at the catchment scale.

Appendix A. Supplementary data

Supplementary data to this article can be found online at
http://dx.doi.org/10.1016/j.scitotenv.2015.03.008.

References

Ahrens B. Distance in spatial interpolation of daily rain gauge data. Hydrol. Earth Syst. Sci. 2006; 10: 197-208.

American Society for Testing and Materials. Standard test methods for determining sediment concentration in water samples: D 3977-97. 11.02, 2000, pp. 395 - 400.

Arnborg L, Walker HJ, Peippo J. Suspended Load in the Colville River, Alaska, 1962. Geografiska Annaler. Series A, Physical Geography 1967; 49: 131-144.

Bača P. Hysteresis effect in suspended sediment concentration in the Rybárik basin, Slovakia. Hydrological Sciences 2008; 53: 224 - 235.

Benda L, Hassan MA, Church M, May CL. Geomorphology of steepland headwaters: The transition from hillslopes to channels. JAWRA Journal of the American Water Resources Association 2005; 41: 835-851.

Bilotta GS, Brazier RE, Haygarth PM. Processes affecting transfer of sediment and colloids, with associated phosphorus, from intensively farmed grasslands: erosion. Hydrological Processes 2007; 21: 135-139.

Bilotta GS, Krueger T, Brazier RE, Butler P, Freer J, Hawkins JMB, et al. Assessing catchment-scale erosion and yields of suspended solids from improved temperate grassland. Journal of Environmental Monitoring 2010; 12: 731-739.

Bishop K, Buffam I, Erlandsson M, Fölster J, Laudon H, Seibert J, et al. Aqua Incognita: the unknown headwaters. Hydrological Processes 2008; 22: 1239 - 1242.

Bogen J. The hysteresis effect of sediment transport (river) systems. Norsk Geografisk Tidsskrift 1980; 34: 45 - 54.

Bowes MJ, House WA, Hodgkinson RA. Phosphorus dynamics along a river continuum. Science of The Total Environment 2003; 313: 199-212.

Bowes MJ, House WA, Hodgkinson RA, Leach DV. Phosphorus–discharge hysteresis during storm events along a river catchment: the River Swale, UK. Water Research 2005; 39: 751-762.

Bracken LJ, Turnbull L, Wainwright J, Bogaart P. Sediment connectivity: a framework for understanding sediment transfer at multiple scales. Earth Surface Processes and Landforms 2014; 40: 177 - 188.

Bull LJ. Magnitude and variation in the contribution of bank erosion to the suspended sediment load of the River Severn, UK. Earth Surface Processes and Landforms 1997; 22: 1109-1123.

Burt TP. Integrated management of sensitive catchment systems. Catena 2001; 42: 275-290.

Carling PA. Particulate dynamics, dissolved and total load, in two small basins, northern Pennines, UK. Hydrological Sciences 1983; 28: 355 - 375.

Chanat JG, Rice KC, Hornberger GM. Consistency of patterns in concentration-discharge plots. Water Resources Research 2002; 38: 22-1-22-10.

Collins AL, Ohandja DG, Hoare D, Voulvoulis N. Implementing the Water Framework Directive: a transition from established monitoring networks in England and Wales. Environmental Science & Policy 2012; 17: 49-61.

Collins AL, Walling DE. Documenting catchment suspended sediment sources: problems, approaches and prospects. Progress in Physical Geography 2004; 28: 159 - 196.

Cotton JA, Wharton G, Bass JAB, Heppell CM, Wotton RS. The effects of seasonal changes to in-stream vegetation cover on patterns of flow and accumulation of sediment. Geomorphology 2006; 77: 320-334.

Cranfield University. The Soils Guide. Cranfield University, 2014.

de Vente J, Poesen J. Predicting soil erosion and sediment yield at the basin scale: Scale issues and semi-quantitative models. Earth-Science Reviews 2005; 71: 95 - 125.

Dean S, Freer J, Beven K, Wade A, Butterfield D. Uncertainty assessment of a process-based integrated catchment model of phosphorus. Stochastic Environmental Research and Risk Assessment 2009; 23: 991-1010.

Deasy C, Brazier RE, Heathwaite AL, Hodgkinson R. Pathways of runoff and sediment transfer in small agricultural catchments. Hydrological Processes 2009; 23: 1349-1358.

Dils RM, Heathwaite AL. The controversial role of tile drainage in phosphorus export from agricultural land. Water Science and Technology 1999; 39: 55-61.

Eder A, Exner-Kittridge M, Strauss P, Blöschl G. Re-suspension of bed sediment in a small stream - results from two flushing experiments. Hydrol. Earth Syst. Sci. 2014; 18: 1043-1052.

Eder A, Strauss P, Krueger T, Quinton JN. Comparative calculation of suspended sediment loads with respect to hysteresis effects (in the Petzenkirchen catchment, Austria). Journal of Hydrology 2010; 389: 168-176.

Elisenreich SJ, Bannerman RT, Armstrong DE. A simplified phosphorus analysis technique. Environ Lett 1975; 9: 43-53.

Ewen J, Geris J, O'Donnell G, Mayes Q, O'Connell E. Multiscale Experimentation, Monitoring and Analysis of Long-term Land Use Changes and Flood Risk - SC060092: Final Science Report. Newcastle University, Newcastle-Upon-Tyne, 2010.

Foster IDL, Chapman AS, Hodgkinson RM, Jones AR, Lees JA, Turner SE, et al. Changing suspended sediment and particulate phosphorus loads and pathways in underdrained lowland agricultural catchments; Herefordshire and Worcestershire, U.K. In: Kronvang B, editor. The Interactions between Sediments and Water. 169. Springer Netherlands, 2003, pp. 119-126.

Giménez R, Casalí J, Grande I, Díez J, Campo MA, Álvarez-Mozos J, et al. Factors controlling sediment export in a small agricultural watershed in Navarre (Spain). Agricultural Water Management 2012; 110: 1-8.

Glendell M, Brazier RE. Accelerated export of sediment and carbon from a landscape under intensive agriculture. Science of The Total Environment 2014; 476–477: 643-656.

Halliday S, Skeffington R, Bowes M, Gozzard E, Newman J, Loewenthal M, et al. The Water Quality of the River Enborne, UK: Observations from High-Frequency Monitoring in a Rural, Lowland River System. Water 2014; 6: 150-180.

Harrington ST, Harrington JR. Dissolved and particulate nutrient transport dynamics of a small Irish catchment: the River Owenabue. Hydrol. Earth Syst. Sci. 2014; 18: 2191-2200.

Hatch LK, Reuter JE, Goldman CR. Daily phosphorus variation in a mountain stream. Water Resources Research 1999; 35: 3783-3791.

Haygarth PM, Condron LM, Heathwaite AL, Turner BL, Harris GP. The phosphorus transfer continuum: Linking source to impact with an interdisciplinary and multi-scaled approach. Science of The Total Environment 2005a; 344: 5-14.

Haygarth PM, Heathwaite AL, Jarvis SC, Harrod TR. Hydrological Factors for Phosphorus Transfer from Agricultural Soils. In: Sparks DL, editor. Advances in Agronomy. Volume 69. Academic Press, 1999, pp. 153-178.

Haygarth PM, Page TJC, Beven KJ, Freer J, Joynes A, Butler P, et al. Scaling up the phosphorus signal from soil hillslopes to headwater catchments. Freshwater Biology 2012; 57: 7-25.

Haygarth PM, Wood FL, Heathwaite AL, Butler PJ. Phosphorus dynamics observed through increasing scales in a nested headwater-to-river channel study. Science of The Total Environment 2005b; 344: 83-106.

Heathwaite AL, Burke SP, Bolton L. Field drains as a route of rapid nutrient export from agricultural land receiving biosolids. Science of The Total Environment 2006; 365: 33-46.

Heathwaite AL, Dils RM. Characterising phosphorus loss in surface and subsurface hydrological pathways. Science of The Total Environment 2000; 251–252: 523-538.

Heathwaite AL, Quinn PF, Hewett CJM. Modelling and managing critical source areas of diffuse pollution from agricultural land using flow connectivity simulation. Journal of Hydrology 2005; 304: 446-461.

Hodgkinson RA, Withers PJA. Sourcing, transport and control of phosphorus loss in two English headwater catchments. Soil Use and Management 2007; 23: 92-103.

Holden J, Shotbolt L, Bonn A, Burt TP, Chapman PJ, Dougill AJ, et al. Environmental change in moorland landscapes. Earth-Science Reviews 2007; 82: 75-100.

Horsburgh JS, Spackman Jones A, Stevens DK, Tarboton DG, Mesner NO. A sensor network for high frequency estimation of water quality constituent fluxes using surrogates. Environmental Modelling & Software 2010; 25: 1031-1044.

Houghton-Carr H. 'Flood Estimation Handbook, Vol. 4' Restatement and application of the Flood Studies Report rainfall-runoff method. Institute of Hydrology, Wallingford, UK, 1999.

Jarvie HP, Withers PJA, Hodgkinson R, Bates A, Neal M, Wickham HD, et al. Influence of rural land use on streamwater nutrients and their ecological significance. Journal of Hydrology 2008; 350: 166-186.

Jordan TE, Whigham DF, Hofmockel KH, Pittek MA. Nutrient and Sediment Removal by a Restored Wetland Receiving Agricultural Runoff. J. Environ. Qual. 2003; 32: 1534-1547.

Kaiser H. The varimax criterion for analytic rotation in factor analysis. Psychometrika 1958; 23: 187-200.

Kaiser H. An index of factorial simplicity. Psychometrika 1974; 39: 31-36.

Kovacs A, Honti M, Zessner M, Eder A, Clement A, Blöschl G. Identification of phosphorus emission hotspots in agricultural catchments. Science of The Total Environment 2012; 433: 74-88.

Langlois JL, Johnson DW, Mehuys GR. Suspended sediment dynamics associated with snowmelt runoff in a small mountain stream of Lake Tahoe (Nevada). Hydrological Processes 2005; 19: 3569-3580.

Lefrançois J, Grimaldi C, Gascuel-Odoux C, Gillet N. Suspended sediment and discharge relationships to identify bank degradation as a main sediment source on small agricultural catchments. Hydrological Processes 2007; 21: 2923 - 2933.

Lexartza-Artza I, Wainwright J. Hydrological connectivity: Linking concepts with practical implications. CATENA 2009; 79: 146-152.

Lexartza-Artza I, Wainwright J. Making connections: changing sediment sources and sinks in an upland catchment. Earth Surface Processes and Landforms 2011; 36: 1090-1104.

Mainstone CP, Dils RM, Withers PJA. Controlling sediment and phosphorus transfer to receiving waters – A strategic management perspective for England and Wales. Journal of Hydrology 2008; 350: 131-143.

Mano V, Nemery J, Belleudy P, Poirel A. Assessment of suspended sediment transport in four alpine watersheds (France): influence of the climatic regime. Hydrological Processes 2009; 23: 777-792.

Marttila H, Kløve B. Dynamics of erosion and suspended sediment transport from drained peatland forestry. Journal of Hydrology 2010; 388: 414-425.

McGonigle DF, Burke SP, Collins AL, Gartner R, Haft MR, Harris RC, et al. Developing Demonstration Test Catchments as a platform for transdisciplinary land management

research in England and Wales. Environmental Science: Processes & Impacts 2014; 16.

McHugh M. Short-term changes in upland soil erosion in England and Wales: 1999 to 2002. Geomorphology 2007; 86: 204-213.

McKee L, Eyre B, Hossain S. Intra- and interannual export of nitrogen and phosphorus in the subtropical Richmond River catchment, Australia. Hydrological Processes 2000; 14: 1787-1809.

Mellander P-E, Melland AR, Jordan P, Wall DP, Murphy PNC, Shortle G. Quantifying nutrient transfer pathways in agricultural catchments using high temporal resolution data. Environmental Science & Policy 2012; 24: 44-57.

Met Office. UKCP09: Average annual rainfall dataset, 2009.

Meyer JL, Strayer DL, Wallance JB, Eggert SL, Helfman GS, Leonard NE. The contribution of headwater streams to biodiversity in river networks. Journal of the American Water Resources Association 2007; 43: 86 - 103.

Naden P. The Fine-Sediment Cascade. In: Burt TP, Allison R, editors. Sediment Cascades: An integrated approach. Wiley & Sons, Chichester, UK, 2010, pp. 471.

Newson M. Understanding 'hot-spot' problems in catchments: the need for scale-sensitive measures and mechanisms to secure effective solutions for river management and conservation. Aquatic Conservation: Marine and Freshwater Ecosystems 2010; 20: S62-S72.

Outram FN, Lloyd CEM, Jonczyk J, Benskin CMH, Grant F, Perks MT, et al. High-frequency monitoring of nitrogen and phosphorus response in three rural catchments to the end of the 2011–2012 drought in England. Hydrol. Earth Syst. Sci. 2014; 18: 3429-3448.

Owen GJ, Perks MT, Benskin CMH, Wilkinson ME, Jonczyk J, Quinn PF. Monitoring agricultural diffuse pollution through a dense monitoring network in the River Eden Demonstration Test Catchment, Cumbria, UK. Area 2012; 44: 443-453.

Pacheco FAL, Varandas SGP, Sanches Fernandes LF, Valle Junior RF. Soil losses in rural watersheds with environmental land use conflicts. Science of The Total Environment 2014; 485–486: 110-120.

Perks MT, Warburton J, Bracken L. Critical assessment and validation of a time-integrating fluvial suspended sediment sampler. Hydrological Processes 2014; 28: 4795-4807.

Pilgrim DH, Huff DD. Suspended sediment in rapid subsurface stormflow on a large field plot. Earth Surface Processes and Landforms 1983; 8: 451-463.

Pionke HB, Gburek WJ, Sharpley AN, Schnabel RR. Flow and nutrient export patterns for an agricultural hill-land watershed. Water Resources Research 1996; 32: 1795-1804.

Posthumus H, Deeks LK, Rickson RJ, Quinton JN. Costs and benefits of erosion control measures in the UK. Soil Use and Management 2013.

Posthumus H, Hewett CJM, Morris J, Quinn PF. Agricultural land use and flood risk management: Engaging with stakeholders in North Yorkshire. Agricultural Water Management 2008; 95: 787-798.

Quinton JN, Govers G, Van Oost K, Bardgett RD. The impact of agricultural soil erosion on biogeochemical cycling. Nature Geosci 2010; 3: 311-314.

Reid SC, Lane SN, Montgomery DR, Brookes CJ. Does hydrological connectivity improve modelling of coarse sediment delivery in upland environments? Geomorphology 2007; 90: 263-282.

Rhea SA, Miller WW, Blank RR, Palmquist DE. Presence and Behavior of Colloidal Nitrogen and Phosphorus in a Sierra Nevada Watershed Soil. J. Environ. Qual. 1996; 25: 1449-1451.

Rodríguez-Blanco ML, Taboada-Castro MM, Taboada-Castro MT. Linking the field to the stream: Soil erosion and sediment yield in a rural catchment, NW Spain. Catena 2010; In Press, Corrected Proof.

Römer W. Concepts for a more efficient use of phosphorus based on experimental observations. Berichte über Landwirtschaft 2009; 87: 5 - 30.

Russell MA, Walling DE, Hodgkinson RA. Suspended sediment sources in two small lowland agricultural catchments in the UK. Journal of Hydrology 2001; 252: 1 - 24.

Sadeghi SHR, Mizuyama T, Miyata S, Gomi T, Kosugi K, Fukushima T, et al. Determinant factors of sediment graphs and rating loops in a reforested watershed. Journal of Hydrology 2008; 356: 271-282.

Sayer AM, Walsh RPD, Bidin K. Pipeflow suspended sediment dynamics and their contribution to stream sediment budgets in small rainforest catchments, Sabah, Malaysia. Forest Ecology and Management 2006; 224: 119-130.

Seeger M, Errea M-P, Beguería S, Arnáez J, Martí C, García-Ruiz JM. Catchment soil moisture and rainfall characteristics as determinant factors for discharge/suspended sediment hysteretic loops in a small headwater catchment in the Spanish Pyrenees. Journal of Hydrology 2004; 288: 299 - 311.

Sharpley AN, Smith SJ, Jones OR, Berg WA, Coleman GA. The Transport of Bioavailable Phosphorus in Agricultural Runoff. J. Environ. Qual. 1992; 21: 30-35.

Shrestha S, Kazama F. Assessment of surface water quality using multivariate statistical techniques: A case study of the Fuji river basin, Japan. Environmental Modelling & Software 2007; 22: 464-475.

Sims JT, Simard RR, Joern BC. Phosphorus Loss in Agricultural Drainage: Historical Perspective and Current Research. J. Environ. Qual. 1998; 27: 277-293.

Singh KP, Malik A, Mohan D, Sinha S. Multivariate statistical techniques for the evaluation of spatial and temporal variations in water quality of Gomti River (India)—a case study. Water Research 2004; 38: 3980-3992.

Siwek J, Siwek JP, Żelazny M. Environmental and land use factors affecting phosphate hysteresis patterns of stream water during flood events (Carpathian Foothills, Poland). Hydrological Processes 2013; 27: 3674-3684.

Sloto RA, Crouse MY. HYSEP: A computer program for streamflow hydrograph separation and analysis. U.S. Geological Survey, 1996, pp. 46.

Smith HG, Dragovich D. Interpreting sediment delivery processes using suspended sediment-discharge hysteresis patterns from nested upland catchments, south-eastern Australia. Hydrological Processes 2009; 23: 2415-2426.

Soulsby C, Gibbins C, Wade AJ, Smart R, Helliwell R. Water quality in the Scottish uplands: a hydrological perspective on catchment hydrochemistry. Science of The Total Environment 2002; 294: 73-94.

Steegen A, Govers G, Nachtergaele J, Takken I, Beuselinck L, Poesen J. Sediment export by water from an agricultural catchment in the Loam Belt of central Belgium. Geomorphology 2000; 33: 25-36.

Sturdee A, Foster I, Bodley-Tickell AT, Archer A. Water quality and Cryptosporidium distribution in an upland water supply catchment, Cumbria, UK. Hydrological Processes 2007; 21: 873-885.

Stutter MI, Langan SJ, Cooper RJ. Spatial contributions of diffuse inputs and within-channel processes to the form of stream water phosphorus over storm events. Journal of Hydrology 2008; 350: 203-214.

Thompson J, Cassidy R, Doody DG, Flynn R. Predicting critical source areas of sediment in headwater catchments. Agriculture, Ecosystems & Environment 2013; 179: 41-52.

Valle Junior RF, Varandas SGP, Pacheco FAL, Pereira VR, Santos CF, Cortes RMV, et al. Impacts of land use conflicts on riverine ecosystems. Land Use Policy 2015; 43: 48-62.

Valle Junior RF, Varandas SGP, Sanches Fernandes LF, Pacheco FAL. Environmental land use conflicts: A threat to soil conservation. Land Use Policy 2014; 41: 172-185.

VanSickle J, Beschta RL. Supply-Based Models of Suspended Sediment Transport in Streams. Water Resources Research 1983; 19: 768 – 778.

Verachtert E, Maetens W, Van Den Eeckhaut M, Poesen J, Deckers J. Soil loss rates due to piping erosion. Earth Surface Processes and Landforms 2011; 36: 1715-1725.

Wade AJ, Palmer-Felgate EJ, Halliday SJ, Skeffington RA, Loewenthal M, Jarvie HP, et al. Hydrochemical processes in lowland rivers: insights from in situ, high-resolution monitoring. Hydrol. Earth Syst. Sci. 2012; 16: 4323-4342.

Webb BW, Walling DE. The magnitude and frequency characteristics of fluvial transport in a Devon drainage basin and some geomorphological implications. Catena 1982; 9: 9 - 23.

Wilkinson ME, Quinn PF, Barber NJ, Jonczyk J. A framework for managing runoff and pollution in the rural landscape using a Catchment Systems Engineering approach. Science of The Total Environment 2013.

Williams GP. Sediment concentration versus water discharge during single hydrologic events in rivers. Journal of Hydrology 1989; 111: 89 - 106.

Withers PJA, Edwards AC, Foy RH. Phosphorus cycling in UK agriculture and implications for phosphorus loss from soil. Soil Use and Management 2001; 17: 139-149.

Withers PJA, Hodgkinson RH, Adamson H, Green G. The impact of pasture improvement on phosphorus concentrations in soils and streams in an upland catchment in Northern England. Agriculture, Ecosystems & Environment 2007; 122: 220-232.

Withers PJA, Jarvie HP. Delivery and cycling of phosphorus in rivers: A review. Science of The Total Environment 2008; 400: 379-395.